

5.5.3 Gain Guiding and Transverse Coherence

Solving the dispersion relation (5.123) is in general not analytically possible. We will discuss numerical approaches to determining the growing FEL eigenvalues and eigenmodes of realistic electron distributions in the next section. Here, however, we present an idealized electron beam model that can be solved exactly, as this will provide useful insight into the general structure of the solutions, along with qualitatively accurate 3D eigenmode profiles and growth rates.

Our simple model will focus on the transverse effects of gain guiding, ignoring the gain degrading effects associated with nonzero emittance and energy spread. Thus, we assume that the electron beam has zero divergence ($\sigma_p = k_\beta = 0$), vanishing energy spread, and a finite transverse envelope $U(\hat{\mathbf{x}})$. In this model the smooth background distribution function is given by

$$\bar{f}_0(\hat{\eta}, \hat{\mathbf{x}}, \hat{\mathbf{p}}) = \delta(\hat{\eta})\delta(\hat{\mathbf{p}})U(\hat{\mathbf{x}}). \quad (5.130)$$

Inserting (5.130) into the dispersion relation (5.123) and changing to the polar coordinates $\hat{r} \equiv |\hat{\mathbf{x}}|$ and $\phi \equiv \tan^{-1}(\hat{y}/\hat{x})$ yields

$$\frac{1}{2} \left[\frac{1}{\hat{r}} \frac{\partial}{\partial \hat{r}} \left(\hat{r} \frac{\partial}{\partial \hat{r}} \right) + \frac{1}{\hat{r}^2} \frac{\partial^2}{\partial \phi^2} \right] \mathcal{A}_\ell(\hat{\mathbf{x}}) + \left[\mu_\ell - \frac{\Delta\nu}{2\rho} - \frac{U(\hat{\mathbf{x}})}{\mu_\ell^2} \right] \mathcal{A}_\ell(\hat{\mathbf{x}}) = 0. \quad (5.131)$$

The equation (5.131) is essentially the 2D Schrödinger equation with complex coefficients, and a few exact solutions exist for certain transverse beam envelopes $U(\hat{\mathbf{x}})$. One example given in the literature [1, 15] is for a finite but uniform (square) distribution. A particularly elegant solution also exists for a parabolic approximation to a Gaussian [16], namely

$$U(\hat{\mathbf{x}}) = 1 - \frac{\hat{r}^2}{2\hat{\sigma}_x^2} = 1 - \frac{|\mathbf{x}|^2}{2\sigma_x^2}. \quad (5.132)$$

Note that we should limit (5.132) to $|\mathbf{x}|^2 < 2\sigma_x^2$ (with $U = 0$ otherwise) to avoid negative currents. However, this significantly complicates the eigenmode equation, and we will show that the eigenmodes obtained using (5.132) equal those of the more physical current distribution when $\hat{\sigma}_x \gg 1$. Furthermore, since the solutions are quite similar and much simpler for finite $\hat{\sigma}_x$, we assume that the quadratic profile is valid everywhere.

For the current profile (5.132), separation of variables in cylindrical coordinates implies that $\mathcal{A}_\ell(\hat{\mathbf{x}}) = \mathcal{A}_{\ell,m}(\hat{r})e^{im\phi}$. We introduce the coordinate $y = i\hat{r}^2/\mu_\ell\hat{\sigma}_x$, noting that $\Re(y) \geq 0$ where (5.131) is valid, namely, for the growing modes with $\Im(\mu) > 0$. Expressing the dispersion relation for the parabolic beam (5.132) in terms of y , we have

$$\left[\frac{\partial}{\partial y} \left(y \frac{\partial}{\partial y} \right) - \frac{m^2}{4y} + \frac{\mu_\ell\hat{\sigma}_x}{2i} \left(\mu_\ell - \frac{\Delta\nu}{2\rho} - \frac{1}{\mu_\ell^2} \right) - \frac{y}{4} \right] \mathcal{A}_{\ell,m}(y) = 0. \quad (5.133)$$

Since the potential is quadratic, this equation is a complex version of the 2D simple harmonic oscillator Schrödinger equation, albeit in different variables, and we only briefly present its solution here. The behavior of the mode at large

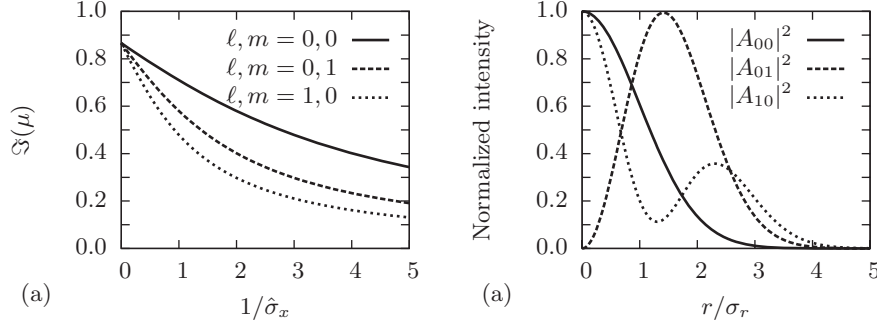


Figure 5.9 Transverse mode structure for the parabolic beam. (a) Growth rate as a function of the inverse of the scaled electron beam size, maximized with respect to $\Delta\nu$. All modes approach the 1D growth rate $\sqrt{3}/2 \approx 0.866$ as $\hat{\sigma}_x \rightarrow \infty$, and decrease as the beam size decreases. The gain of the lowest order Gaussian mode G_{00} decreases the slowest, so that at finite beam size it tends to dominate the other transverse modes. In panel (b) we plot the intensity profile of the three lowest order modes, each being normalized to its peak value with $\hat{\sigma}_x \gg 1$. The mode shapes look quite similar to those shown in Fig. 5.10, which were numerically computed for the LCLS.

y can be easily determined from (5.133), being given by $\mathcal{A}' = \mathcal{A}/4$, so that $\mathcal{A} \sim e^{-y/2}$ in the limit $|y| \rightarrow \infty$. To put the eigenmode equation (5.133) in standard form, we extract the exponential dependence and eliminate the term $\sim m^2/4y$ by defining $\alpha_{\ell,m}(y)$ via

$$\mathcal{A}_{\ell,m}(y) = y^{m/2} e^{-y/2} \alpha_{\ell,m}(y). \quad (5.134)$$

Using this definition results in Laguerre's differential equation for the field $\alpha_{\ell,m}(y)$:

$$y \alpha_{\ell,m}''(y) + (1 + m - y) \alpha_{\ell,m}'(y) - \frac{1}{2} \left[m + 1 + i\mu_\ell \hat{\sigma}_x \left(\mu_\ell - \frac{\Delta\nu}{2\rho} - \frac{1}{\mu_\ell^2} \right) \right] \alpha_{\ell,m}(y) = 0. \quad (5.135)$$

The only non-singular solution for integer m is the generalized Laguerre function, $\alpha_{\ell,m}(y) = L_\ell^m(y)$, where -2ℓ is equal to the term in square brackets from (5.135). Note that $L_\ell^m(y) \sim e^y/y^{\ell+m+1}$ if ℓ is not a positive integer, in which case the field \mathcal{A} would diverge exponentially ($\sim e^{y/2}$) at infinity. Thus, requiring bounded solutions implies that ℓ is a nonnegative integer, meaning that the eigenvalue μ_ℓ must satisfy

$$\mu_\ell^2 \left(\mu_\ell - \frac{\Delta\nu}{2\rho} \right) - 1 = \frac{i\mu_\ell}{\hat{\sigma}_x} (2\ell + m + 1), \text{ for } \ell \geq 0, \ell \in \mathbb{Z} \text{ and } m \in \mathbb{Z}. \quad (5.136)$$

We plot the growth rates for several mode numbers as a function of $1/\hat{\sigma}_x$ in Fig. 5.9(a). Note that as $\hat{\sigma}_x \rightarrow \infty$, the growth rates for all modes become degenerate, with each satisfying the cold, 1D dispersion relation. The eigenmodes

themselves are given by the Gauss-Laguerre functions

$$\mathcal{A}_{\ell,m}(\hat{r}) = \left(\frac{i\hat{r}^2}{\mu_\ell \hat{\sigma}_x} \right)^{m/2} L_\ell^m \left(\frac{i\hat{r}^2}{\mu_\ell \hat{\sigma}_x} \right) \exp \left(-\frac{i\hat{r}^2}{2\mu_\ell \hat{\sigma}_x} \right). \quad (5.137)$$

Figure 5.9(b) shows a few of the lowest-order modes. The rms width of the fundamental mode $\mathcal{A}_{0,0}$ can be easily determined using $|\mathcal{A}_{0,0}|^2 \propto e^{-r^2/2\sigma_r^2}$; we have

$$\sigma_r^2 = \frac{|\mu_\ell|^2 \sigma_x}{2\Im(\mu_\ell) \sqrt{2\rho k_1 k_u}}, \quad (5.138)$$

and the radiation mode size is proportional to the geometric mean of the FEL mode size $\sim (\rho k_1 k_u)^{-1/2}$ and the electron beam size σ_x . Thus, for sufficiently large electron beams that satisfy $\hat{\sigma}_x \gg 1$, the radiation modes have $\sigma_r \ll \sigma_x$. In this limit our parabolic approximation Eq. (5.132) is valid even though the current is negative when $|\hat{\mathbf{x}}|^2 > 2\sigma_x^2$, and we find that the low-order Gauss-Laguerre eigenmodes (5.137) and growth rates (5.136) are nearly identical to those of a completely non-negative current density.

5.5.4 Numerically Solving the Dispersion Relation

Computing the growing FEL modes including non-zero emittance and energy spread requires a more general approach. In the next section we write down semi-analytic, approximate solutions using the variational technique. Here, on the other hand, we present a numerical method for solving the dispersion relation (5.123). To facilitate these analyses, we open this section by simplifying (5.123), after which we discuss how one can numerically solve the resulting equation.

To solve the dispersion relation Eq. (5.123), we first make a change of variable

$$\hat{\mathbf{x}}' = \hat{\mathbf{x}} \cos(\hat{k}_\beta \tau) + \frac{\hat{\mathbf{p}}}{\hat{k}_\beta} \sin(\hat{k}_\beta \tau), \quad (5.139)$$

which is accompanied by the following transformations

$$d\hat{\mathbf{p}} = d\hat{\mathbf{x}}' \frac{\hat{k}_\beta^2}{\sin^2(\hat{k}_\beta \tau)},$$

$$\hat{\mathbf{p}}^2 + \hat{k}_\beta^2 \hat{\mathbf{x}}^2 = \frac{\hat{k}_\beta^2}{\sin^2(\hat{k}_\beta \tau)} \left[\hat{\mathbf{x}}^2 + \hat{\mathbf{x}}'^2 - 2\hat{\mathbf{x}} \cdot \hat{\mathbf{x}}' \cos(\hat{k}_\beta \tau) \right].$$

Equation (5.123) then becomes

$$\left(\mu - \frac{\Delta\nu}{2\rho} + \frac{1}{2} \hat{\nabla}_\perp^2 \right) \mathcal{A}(\hat{\mathbf{x}}) - \int_{-\infty}^0 d\tau \frac{\tau e^{-\hat{\sigma}_n^2 \tau^2 / 2 - i\mu\tau}}{2\pi \hat{\sigma}_x^2 \sin^2(\hat{k}_\beta \tau)} \int d\hat{\mathbf{x}}' \mathcal{A}(\hat{\mathbf{x}}')$$

$$\times \exp \left[-\frac{1 + i\hat{k}_\beta^2 \hat{\sigma}_x^2 \tau}{2\hat{\sigma}_x^2} \frac{\hat{\mathbf{x}}^2 + \hat{\mathbf{x}}'^2 - 2\hat{\mathbf{x}} \cdot \hat{\mathbf{x}}' \cos(\hat{k}_\beta \tau)}{\sin^2(\hat{k}_\beta \tau)} \right] = 0.$$